

Original Article

Corresponding Author

Jianwen Xu


 <https://orcid.org/0000-0002-8095-591X>

Department of Rehabilitation Medicine,
First Affiliated Hospital, Guangxi Medical
University, 6 Shuangyong Road, Nanning
530021, China

Email: xujianwen@gxmu.edu.cn

Co-corresponding Author

Jianmin Chen

 <https://orcid.org/0000-0002-0528-5354>

Department of Rehabilitation Medicine,
First Affiliated Hospital, Fujian
Medical University, 20 Chazhong Road,
Fuzhou 350004, China

Email: cjm625@163.com

Received: April 11, 2023

Revised: June 24, 2023

Accepted: July 7, 2023

*Shuhui Guo and Jianmin Chen
contributed equally to this study as
co-first authors.



This is an Open Access article distributed under the terms of the Creative Commons Attribution Non-Commercial License (<https://creativecommons.org/licenses/by-nc/4.0/>) which permits unrestricted non-commercial use, distribution, and reproduction in any medium, provided the original work is properly cited.

Copyright © 2023 by the Korean Spinal
Neurosurgery Society

INTRODUCTION

A spinal cord injury (SCI) is an extremely serious neurological event characterized by permanent disability in the body below the injured region. The affected individual's resulting inability to work (labor) and the costs of long-term treatment impose

Electroacupuncture-Modulated MiR-106b-5p Expression Enhances Autophagy by Targeting Beclin-1 to Promote Motor Function Recovery After Spinal Cord Injury in Rats

Shuhui Guo^{1,*}, Jianmin Chen^{2,*}, Ye Yang¹, Xiaolu Li¹, Yun Tang¹, Yuchang Gui¹, Jianquan Chen³, Jianwen Xu¹

¹Department of Rehabilitation Medicine, The First Affiliated Hospital of Guangxi Medical University, Guangxi, China

²Department of Rehabilitation Medicine, The First Affiliated Hospital of Fujian Medical University, Fujian, China

³Department of Orthopedics, The First Affiliated Hospital of Guangxi University of Chinese Medicine, Guangxi, China

Objective: Electroacupuncture (EA) has a definite effect on the treatment of spinal cord injuries (SCIs), but its underlying molecular mechanism remains unclear. Meanwhile, MiR-106b-5p is an autophagy- and apoptosis-related microribonucleic acid, but whether it regulates the progression of autophagy and apoptosis in SCIs is yet undetermined. As such, this study aimed to elucidate the involvement of miR-106b-5p in the EA treatment of an SCI.

Methods: The miR-106b-5p level was detected by quantitative real-time polymerase chain reaction. *In vitro*, SH-SY5Y cells were transfected with miR-106b-5p mimics or inhibitors to regulate the miR-106b-5p expression, while *in vivo*, SCI rats were treated with EA for 7 days at the bilateral Zusanli (ST36) and Jiaji (EX-B2) acupoints. The motor function was evaluated using the Basso-Beattie-Bresnahan (BBB) criteria. Further, autophagic vacuoles, pathological damage, and neuronal cell morphology were observed by transmission electron microscopy, as well as by hematoxylin and eosin and Nissl staining, respectively.

Results: The miR-106b-5p level, which can interact directly with Beclin-1 by influencing its expression, as well as the expressions of P62, Caspase-3, and Bax, was upregulated after an SCI, but it decreased after EA. Moreover, the ratio of LC3-II to LC3-I was upregulated after EA. EA can enhance autophagy, reduce neuronal apoptosis, and minimize motor dysfunction and histopathological deficits after an SCI. More importantly, however, all the above effects induced by EA can be reversed after an injection of miR-106-5p agomir to produce an overexpression of miR-106b-5p.

Conclusion: EA treatment could downregulate miR-106b-5p to alleviate SCI-mediated injuries by promoting autophagy and inhibiting apoptosis.

Keywords: Spinal cord injury, Electroacupuncture, Autophagy, Apoptosis

a heavy financial burden on their family and the wider community.¹ Despite concerted efforts focused on SCIs in global terms, no effective breakthrough has yet been made toward a cure for the neurological dysfunction caused by an SCI.^{2,3} Thus, it is imperative to further explore the pathophysiological mechanism of and to develop effective rehabilitation strategies for SCIs.⁴

The pathophysiological progression of an SCI is generally included 2 phases: primary injury and secondary injury.⁵ The primary injury leads to irreversible neuronal damage to the spinal cord. The secondary injury, including apoptosis, autophagy, inflammation and so on, that jointly result in tissue destruction and microenvironment changes in the SCI region and lead to nerve repair difficulties.^{4,6} Autophagy is a catabolic process designed to maintain cell homeostasis by degrading cytoplasmic components and organelles in lysosomes, and the inhibition of autophagic flux after an SCI can lead to a poorer functional recovery.⁷ Meanwhile, apoptosis is a leading cause of neurological dysfunction and death after an SCI, but appropriate autophagy activation can act as a protective mechanism against the apoptosis of neuronal cells and can provide a favorable microenvironment for nerve regeneration after an SCI. Some researchers believe autophagy is a potential therapeutic target of SCIs.⁸ Thus, the adoption of rehabilitation strategies capable of halting apoptosis and activating autophagy during the secondary injury is crucial to limiting the spread of secondary damage, affecting nerve regeneration positively, and promoting functional recovery.⁹

Electroacupuncture (EA) is a therapy derived from traditional Chinese medicine that involves the insertion of sterile, single-use needles into acupoints according to a system of meridians and the application of an electrical current through the needles.^{10,11} The utilization of EA to alleviate pathological damage and improve functional recovery in the treatment of SCIs has gained much popularity in recent years.^{4,11} With fundamental studies having indicated that EA can promote nerve repair and increase motor outcomes by regulating cell autophagy and apoptosis post-SCI.¹² For example, Liu and Wu¹³ performed a microarray analysis of SCI samples and EA-induced SCI samples harvested at 7, 14, and 28 days, revealing that a large set of microribonucleic acids (miRNAs) had altered expressions upon EA treatment. Thus, EA may exert therapeutic effects against motor dysfunction in SCIs by modulating miRNA expression profiles.

MiRNAs are a class of endogenous, noncoding, small RNAs with 22–24 nucleotides working as master administrative molecules to regulate gene expressions. This is achieved by binding to the 3' or 5' untranslated regions of the target messenger RNA (mRNA) to inhibit translation and induce degradation.⁸ Though relatively small in number, miRNAs are believed to be involved in multiple specific biological activities in the body and to play a crucial role in the modulation of secondary injury after an SCI.¹⁴ For example, He et al. observed that the overexpression of miR-92a-3p can promote neurological recovery by inhibiting cell apoptosis in mice with SCIs.¹⁵ Further, Zhou et al.¹⁶ concluded

that blocking the expression of miR-378-3p can increase cell viability by regulating apoptosis and autophagy in *in vitro* SCI models. Thus, certain miRNAs represent potential promising therapeutic targets for SCI repair.¹⁷ To date, the aberrant miR-106b-5p expression has been implicated in many neurological disorders, and it leads to abnormal cell apoptosis and autophagy.^{18–20} However, the role of miR-106b-5p in SCI remains unclear, warranting further investigation. Therefore, we aimed to explore the relationship between the miR-106b-5p expression and EA treatment of SCIs and, furthermore, to validate the speculation that the regulation of apoptosis and autophagy might be responsible for the EA-mediated repair of motor function via downregulation of the miR-106b-5p expression.

MATERIALS AND METHODS

1. SCI Patients

Patients with an SCI (n = 10) were enrolled between December 2022 and January 2023 from the Department of Rehabilitation Medicine of the First Affiliated Hospital of Guangxi Medical University. Inclusion criteria were as follows: an age of ≥ 18 years, a first-time SCI, a disease duration of less than one year, and a motor-incomplete injury.¹⁸ Another 10 healthy volunteers without evidence of an SCI were selected as controls during the same period and were age- and sex-matched with the patients. The exclusion criteria were as follows: a previous history of neurological disease, renal dysfunction, severe liver disease, a known or suspected malignancy, surgery, or a skeletal muscle injury within the previous 6 month.¹⁹ Samples of about 5 mL of venous blood were taken from each participant via ethylenediamine-tetraacetic acid anticoagulant tubes (Sanli, Liuyang, China) in the morning after 12 hours of fasting. All participants gave their written informed consent to participate in this study, and all procedures performed involving human participants were conducted in accordance with the Declaration of Helsinki and approved by the Ethics Committee of the First Affiliated Hospital of Guangxi Medical University (approval number: 2022-K143-01). The chictcr.org identifier is ChiCTR2200066985 (<https://www.chictcr.org.cn/edit.aspx?pid=186333&html=4>). The animal experimental protocol was approved by the Guangxi Medical University Animal Research Ethics.

2. Luciferase Reporter Assay

A bioinformatics analysis was performed using BiBiServ (<https://bibiserv.cebitec.unibielefeld.de/rnahybrid>) to identify a favorable binding site between miR-106b-5p and Beclin-1. The

sequences of Beclin-1 3'UTR fragments containing a wild-type (WT) or mutant (Mut) binding site of miR-106b-5p were ordered and synthesized by GeneChem (Shanghai, China), and the GV272 vector (GeneChem) was used to construct the Beclin-1-WT and Beclin-1-MUT recombinant vectors. HEK-293T cells (2×10^4 cells/well) were seeded in 24-well plates followed by cotransfection with p-miR-Beclin-1 3'UTR, p-miR-Beclin-1-mutant-3'UTR, and miR-106b-5p mimics or a negative control (NC) using Lipofectamine 2000 (Invitrogen, Carlsbad, CA, USA). Luciferase activity was assessed 48 hours after transfection using a Dual-Luciferase Assay System (Promega, Madison, WI, USA) and normalized according to Renilla luciferase activity (GeneChem).

3. Cell Culture and Transfection

The human neuroblastoma cell line, SH-SY5Y, is a commonly used tool in human *in vitro* SCI research²¹; herein, SH-SY5Y cells were purchased from the Shanghai Cell Bank of the Chinese Academy of Sciences (Shanghai, China) and maintained per their guidelines. The cells were stored at 37°C and 5% CO₂ in Dulbecco Modified Eagle's Medium (DMEM; Gibco, Carlsbad, CA, USA) supplemented with 8% fetal bovine serum (FBS; Gibco) and a 1% penicillin-streptomycin-mixed solution (Gibco). The SH-SY5Y cells were randomly distributed into the following 4 groups: (1) an miR-106b-5p mimic group, (2) a NC mimic group, (3) a miR-106b-5p inhibitor group, and (4) an NC inhibitor group. For miRNA transfection, cells were seeded in a six-well plate at 3×10^5 cells per well and transiently transfected 1 d later using Lipofectamine 3000 (Invitrogen) in the OptiMEM medium (Invitrogen) according to the manufacturer's instructions (Fig. 1A). Moreover, miR-106b-5p mimics and inhibitors, along with their corresponding NC mimics and NC inhibitors, were purchased from Bioneer Corporation (Shanghai, China).

4. Experimental Animals and SCI Model

Adult female Sprague Dawley rats (8 weeks old, 200–220 g) were purchased from the Animal Experimental Center (Guangxi Medical University, Nanning, China), all of which were housed in a specific pathogen-free environment at 22°C–24°C with available food and water. The Guangxi Medical University Animal Research Ethics Committee (approval No. 202209002) approved the ethics application concerning animal protocols. The rats were randomized into a sham group, SCI group, SCI+EA group, SCI+EA+miR-106b-5p agomir group, and SCI+EA+miR-106b-5P NC group, and random numbers were generated using the

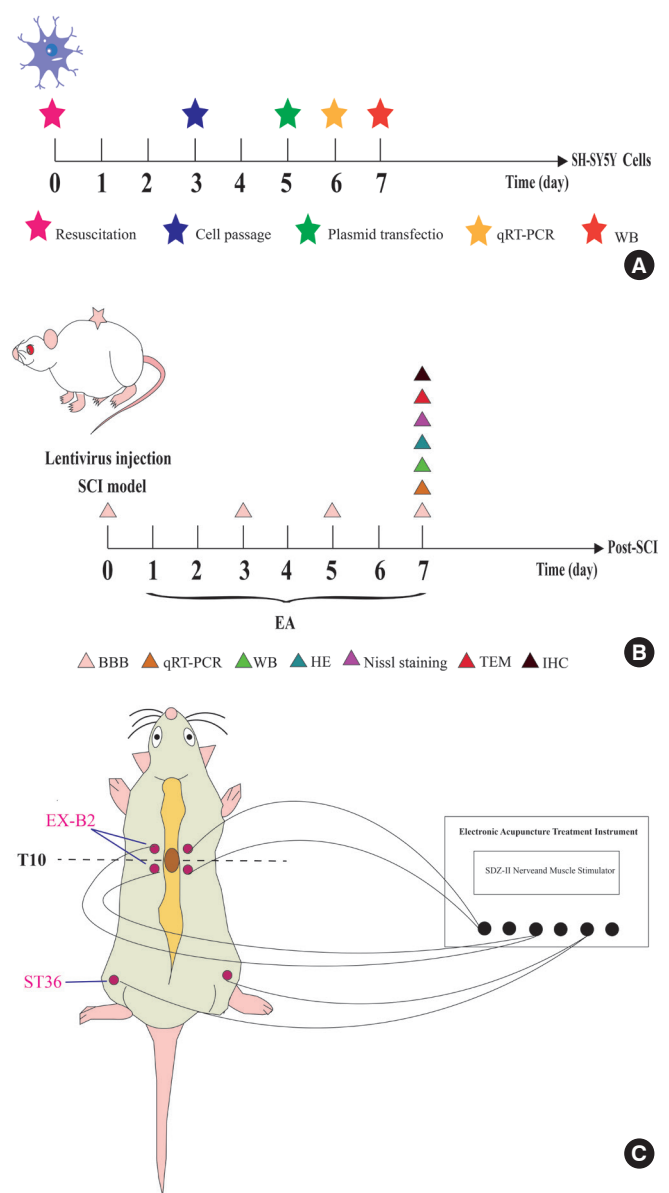


Fig. 1. The schematic diagram illustrating the chronological events of experiments. (A) The schematic diagram for experiments *in vitro*. (B) The schematic diagram for experiments *in vivo*. (C) Rat schematic showing the location of the EA acupoints selected in the present study. ST36 stands for “Zusanli” and EX-B2 stands for “Jiaji”. qRT-PCR, quantitative real-time polymerase chain reaction; WB, Western blot; SCI, spinal cord injury; EA, electroacupuncture; BBB, Basso-Beattie-Bresnahan locomotor scale; HE, hematoxylin and eosin; TEM, transmission electron microscopy; IHC, immunohistochemistry.

RAND function in Microsoft Excel (Microsoft Corp., Albuquerque, NM, USA). In total, 130 rats were used in this study.

The SCI model was established based on a modified Allen's method,^{4,22} and the rats were intraperitoneally (i.p.) injected with

pentobarbital (1%, 50 mg/kg) to create sufficient anesthesia, followed by a laminectomy at T10 to expose the spinal cord completely. Thereafter, the rats were fixed to the stereotaxic apparatus (Ruiwode Life Science Co., Ltd., Shenzhen, China) with the back facing upward. A 10-g impact rod with a 3-mm diameter was dropped from a vertical height of 5 cm through a glass tube, directly impacting the dura mater and spinal cord, with the striking force on the latter measuring 50 gf.cm. The SCI model was successfully constructed, as indicated by the observable hyperemia on the spinal cord surface surrounding the lesion site, spasmodic tail flicks, transient twitches of the body and lower limbs, and sluggish movement or hindlimb paralysis.²³

The rats in the sham group received a partial laminectomy of the T10 vertebrae and the dura was opened, but no contusion was performed. Subsequently, the rats in the SCI+EA+miR-106b-5p agomir and SCI+EA+miR-106b-5P NC groups received 5 μ L of lentivirus vectors (about 4×10^8 TU LV-miR-106b-5p agomir or LV-miR-106b-5p-NC) at 2.5 mm caudal and rostral to the spinal cord lesion (2.5 μ L at each point). After injection, the 10- μ L microliter syringe (Gaoge, Shanghai, China) was left in for 5 minutes and then removed at a speed of 1 mm/min to avoid re-gurgitation of the injected material.^{24,25} All rats were injected with penicillin (80,000 U/d) i.p. after the operation and then once daily for 3 days. Manual bladder expression was performed twice daily in all SCI rats until the bladder was emptied. Finally, lentivirus was constructed by GeneChem Biomedical Co., Ltd. (Shanghai, China), and its titer was determined, where the original lentiviral vector titers for agomir contained 7×10^8 transduction units (TU)/mL and the NC ones 1×10^9 TU/mL (Fig. 1B).

5. Evaluation of Locomotor Capacity

Functional recovery of the hindlimbs in rats was evaluated using the Basso-Beattie-Bresnahan (BBB) scale,²⁶ the scores of which ranged from 0 (complete paralysis) to 21 points (normal locomotion). Briefly, the rats were dynamically evaluated using the scale at 1, 3, 5, and 7 days after surgery in an open field for more than 5 minutes, where a 1-day postsurgery BBB score of greater than 3 would suggest failed modeling. The rats that failed the modeling were excluded, and backup rats were used as a modeling supplement. In addition, all rats were evaluated before inducing SCIs to ensure no baseline defects. The scale was scored by 2 well-trained, independent raters blinded to the treatment condition.

6. EA Treatment

The day after modeling, all rats in the SCI+EA, SCI+EA+miR-

106b-5p agomir, and SCI+EA+miR-106b-5P NC groups underwent an EA stimulus procedure at the Jiaji and Zusanli acupoints along the T9/T11 levels (EX-B2, bilaterally on the spinous process of the back, and ST36, bilaterally on the hindlimbs below the fibular head by 5 mm, respectively).^{8,9} Disposable, sterilized stainless-steel acupuncture needles sized 0.25×25 mm (Huatuo, Suzhou Medical Co., Ltd., Jiangsu, China) were inserted to a depth of 4–5 mm, until the tip made contact with the vertebral lamina. Then, the needles were connected to the Hua Tuo acupoint neurostimulator (Model SDZ-II EA, Suzhou Medical Co., Ltd.) using 3 pairs of electrodes. The stimulation parameters were set as sparse-dense waves of 2 Hz for 20 min/day at a 0.5-mA intensity once daily for 7 days.²³ Meanwhile, the rats in the SCI and sham groups underwent prone positioning without EA treatment for 20 minutes (Fig. 1C).

7. Hematoxylin and Eosin and Nissl Staining

A 10-mm section of the injured spinal cord tissue, at the epicenter of the injury site, was carefully harvested on the seventh day after surgery. The sample was fixed in 4% paraformaldehyde for 24 hours and embedded in paraffin, and cross-sections (4- μ m thick) were made on slides with a poly-L-lysine coating for the analysis of diseased tissue based on hematoxylin and eosin (H&E) and Nissl staining, after being deparaffinized and rehydrated. An optical microscope (BX53, Olympus, Tokyo, Japan) was used to capture images.

8. Transmission Electron Microscopy

The fresh spinal cord samples from T10 were harvested and prefixed in 2.5% glutaraldehyde at 4°C for overnight fixation. Then, the samples were sequentially washed, fixed, dehydrated, and soaked in a 1:1 epoxy resin mixture and pure acetone at 40°C for 6 hours. Hereafter, they were embedded in pure epoxy resin at 40°C for 4 hours and then embedded. Ultrathin sections (60 nm) were prepared and double-stained with uranyl acetate (2%) and lead citrate (1%). After rinsing 3 times with double-distilled water, the ultrastructural evaluation of the mitochondria was observed using TEM (HT7800; Hitachi, Tokyo, Japan).

9. RNA Extraction and Quantitative Real-Time Polymerase Chain Reaction

Total RNA in tissues or cells was extracted using a NucleoZol RNA reagent (Macherey-Nagel, Duren, Germany), and complementary DNA was synthesized according to the instructions of the RNA polymerase chain reaction (PCR) kit (code no. 638315 or code no. RR036A, Takara, Japan). A PCR reaction was achi-

eved using TB Green Premix Ex Taq II (code no. RR820A, Takara) on the Applied Biosystems StepOne fluorescence quantitative PCR instrument (Applied Biosystems, Waltham, MA, USA). Further, GAPDH/U6 was employed as the internal control, while the $2^{-\Delta\Delta C_t}$ methods were utilized to calculate the relative gene expression. The primer sequences are listed in Supplementary Table 1.

10. Western Blot Test

Total protein in tissues and cells was extracted using radio immunoprecipitation assay buffer (89900, Thermo Fisher Scientific Inc., Waltham, MA, USA). Furthermore, equal amounts of protein from each sample were separated on 12% sodium dodecyl sulfate-polyacrylamide gel electrophoresis gels and transferred to polyvinyl difluoride membranes (Immobilon-PSQ, Merck, Burlington, MA, USA) blocked with 5% nonfat milk in tris-buffered saline containing 0.1% Tween 20 (TBST; TA-125-TT, Thermo Fisher Scientific Inc.) at room temperature for 1 hour and then incubated overnight at 4°C with the following primary antibodies: rabbit LC3B (1:1,000; Abmart, Shanghai, China), rabbit Caspase-3 (1:1,000; Proteintech, Wuhan, China), rabbit p62 (1:1,000; Proteintech), rabbit Bax (1:5,000; Proteintech), rabbit Beclin-1 (1:5,000; Proteintech), rabbit Tubulin (1:5,000; Proteintech), and rabbit GAPDH (1:5,000; Proteintech), the latter 2 of which served as internal loading controls to normalize protein expressions. The following day, the membrane was incubated at room temperature for 1 hour with a secondary antibody (goat anti-rabbit IgG, 1:15,000, Proteintech) and subjected to gentle rocking. Finally, the blots were scanned with a LiCor Odyssey scanner and analyzed using the Odyssey 3.0 analytic software (LiCor, Lincoln, NE, USA).

11. Immunohistochemistry

The slices were permeabilized with 0.2% Triton X-100 (Solarbio, Beijing, China) for 10 minutes, blocked with a blocking buffer (5% FBS in 0.2% Triton X-100) for 1 hour, and washed thrice with phosphate-buffered saline (PBS) for 5 minutes each. Then, the slices were incubated with the primary antibodies P62 (1:100, ABclonal, Wuhan, China), Beclin-1 (1:100, Proteintech), Bax (1:1,000, Proteintech), and Caspase-3 (1:100, Abmart). After washing thrice with PBS, samples were treated with a goat anti-rabbit/mouse monoclonal secondary antibody (ZSGB-BIO, Beijing, China) at 37°C for 30 minutes, and the appropriate amount of freshly prepared 3,3'-diaminobenzidine chromogenic solution and incubate was added at room temperature for 5 minutes. Thereafter, the sections were counterstained with hematoxylin

for 3 minutes and attached to coverslips. Photographic results were taken using an optical microscope (BX53, Olympus).

12. Statistical Analyses

Data analysis and plotting were performed with the IBM SPSS Statistics ver. 25.0 (IBM Co., Armonk, NY, USA) and GraphPad Prism 8.0 (GraphPad Software, La Jolla, CA, USA), respectively. Normally distributed variables are presented as mean \pm standard errors. Comparisons between the 2 groups were achieved using independent samples t-test, and chi-square test, as appropriate. Further, multiple group comparisons were analyzed by 1-way analysis of variance coupled with a least significant difference or Dunnett *post hoc* test, as appropriate (depending on the results of the homogeneity of variance test). All *in vitro* and *in vivo* assays were repeated at least thrice, all statistical tests were 2-tailed, and analysis results with $p < 0.05$ were assumed to be statistically significant.

RESULTS

1. MiR-106b-5p Is Upregulated in SCI Patients' Blood and Rat SCI Model Spinal Tissue

MiR-106b-5p levels were measured in the blood of SCI patients ($n = 10$) and healthy controls ($n = 10$), though the demographic and clinical data did not differ between the 2 groups (Table 1, Supplementary Table 2). A quantitative real-time PCR (qRT-PCR) analysis suggested that miR-106b-5p levels were upregulated in the blood of SCI patients compared to healthy controls ($p < 0.01$) (Fig. 2A), and the expression of miR-106b-5p in the spinal cords of rats at 1-, 3-, 7-, and 14-day postsurgery was significantly increased in the SCI group compared to the sham group ($p < 0.01$) (Fig. 2B).

2. Beclin-1 Is a Direct Target of MiR-106b-5p

To study the relationship between miR-106b-5p and Beclin-1, we first utilized bioinformatics to analyze the nucleotide sequences, and the results showed that miR-106b-5p could potentially bind to the 3'-UTR of Beclin-1 (Fig. 3a). Next, to confirm this, we performed a dual-luciferase reporter assay, and based on the

Table 1. Demographic and clinical data

Parameter	SCI patient	Healthy control	p-value
Sex, male:female	7:3	7:3	1.00
Age (yr)	38.4 \pm 13.95	36.2 \pm 12.94	0.73

Values are presented as number or mean \pm standard deviation. SCI, spinal cord injury.

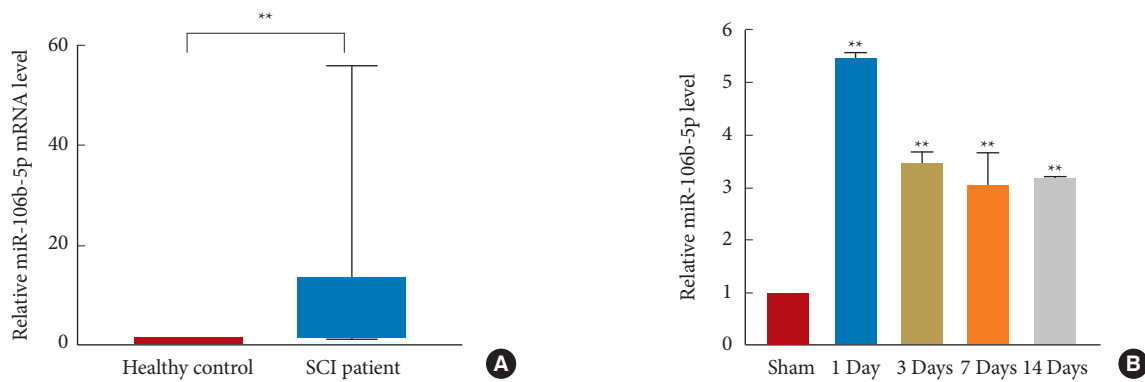


Fig. 2. MiR-106b-5p was highly expressed in spinal cord injuries (SCIs). (A) The expression level of miR-106b-5p in the blood of SCI patients (n = 10) was significantly higher than that in healthy controls (n = 10). (B) The miR-106b-5p level in the spinal cord tissue of the SCI group at 1-, 3-, 7-, and 14-day postsurgery was higher than that in the sham group (n = 6/group). Data are expressed as the mean ± standard deviation, and differences between each group were compared by Student t-test. All experiments were repeated at least thrice. **p < 0.01.

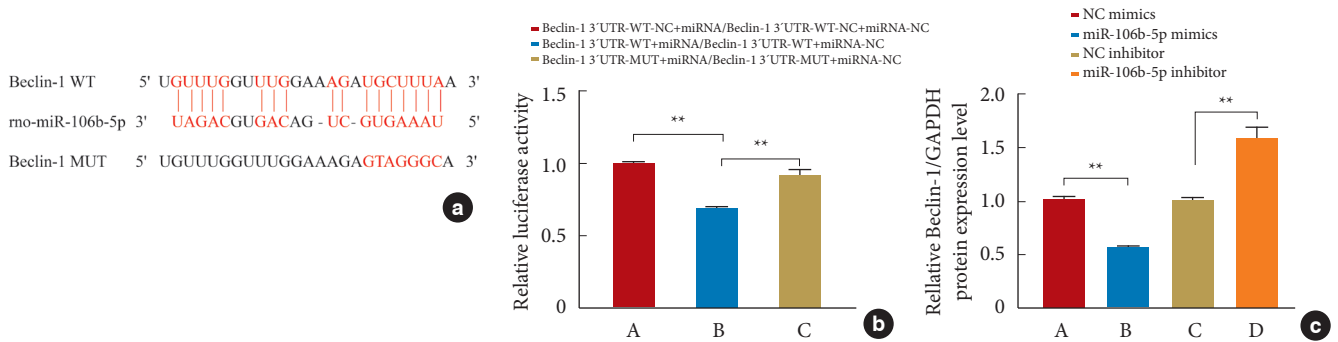


Fig. 3. Beclin-1 was the target gene of miR-106b-5p. (a) Potential binding sites between Beclin-1 and miR-106b-5p. (b) Luciferase activity markedly increased in cells both cotransfected with miR-106b-5p mimics and Beclin-1-WT-NC and cotransfected with miR-106b-5p mimics and Beclin-1-MUT. (c) The relative expression of Beclin-1 mRNA was determined by qRT-PCR in SH-SY5Y cells following transfection with miR-106b-5p mimics/NC mimics and inhibitors. One-way analysis of variance and the LSD multiple comparisons test were used in panel B, and the Student t-test was used in panel C. All results are shown as the mean ± standard deviation (n = 3/group), and all experiments were repeated at least thrice. qRT-PCR, quantitative real-time polymerase chain reaction; NC, negatively control; WT, wild type; MUT, mutant. **p < 0.01.

binding sequences, Beclin-1-WT and Beclin-1-MUT were constructed. Compared with miR-106b-5p mimics and Beclin-1-WT, the luciferase activity markedly increased in cells cotransfected with miR-106b-5p mimics and Beclin-1-WT-NC (p < 0.01) or in cells cotransfected with miR-106b-5p mimics and Beclin-1-MUT (p < 0.01) (Fig. 3b). Meanwhile, the qRT-PCR results showed that the Beclin-1 expression was negatively regulated by miR-106b-5p (Fig. 3c), supporting the notion that miR-106b-5p directly targets Beclin-1.

3. MiR-106b-5p Affects SH-SY5Y Cell Autophagy and Apoptosis *In Vitro*

In vitro, miR-106b-5p mimics/NC mimics and miR-106b-5p inhibitors/NC inhibitors were transfected into SH-SY5Y cells,

respectively, the efficiency of which was assessed by qRT-PCR, which detected the miR-106b-5p expression. As a result, the transfection of miR-106b-5p mimics dramatically increased the expression level of miR-106b-5p (p < 0.01), though it was significantly decreased after transfection with the miR-106b-5p inhibitors (p < 0.01) (Fig. 4a). Subsequently, Western blot (WB) assay findings revealed that the ratio of LC3-II to LC3-I and the expression of Beclin-1 were upregulated, while the expressions of P62, Bax, and Caspase-3 were downregulated in the miR-106b-5p inhibitor group compared with the NC inhibitor group; the opposite results were found in the miR-106b-5p mimic group compared to the NC mimic group (p < 0.05) (Fig. 4b–g).

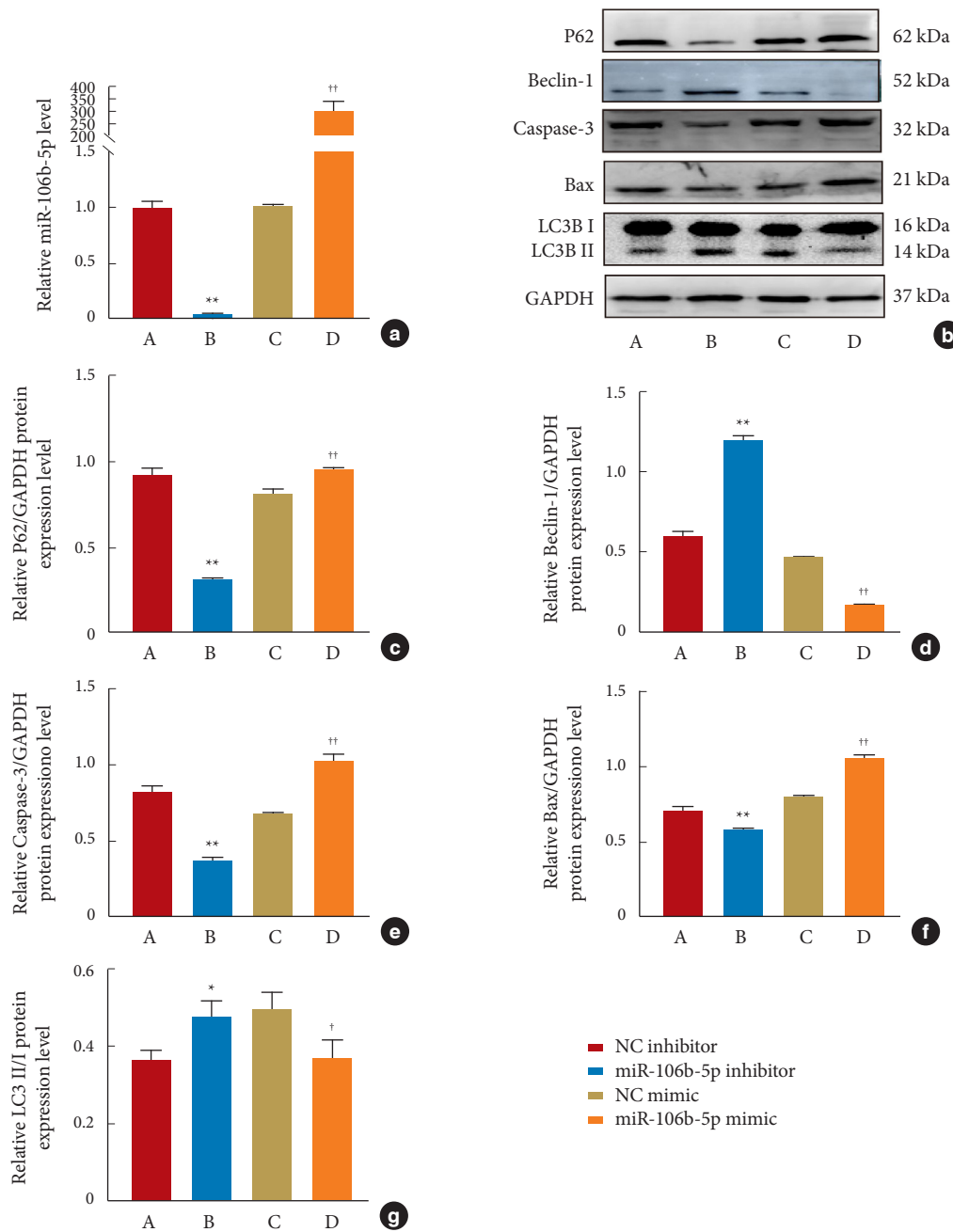


Fig. 4. MiR-106b-5p regulated the expressions of autophagy and apoptosis proteins *in vitro*. (a) A qRT-PCR analysis determined the expression of miR-106b-5p in SH-SY5Y cells transfected with miR-106b-5p mimics/NC mimics and miR-106b-5p inhibitors/NC inhibitors. (b–g) Representative Western blot (WB) bands and the corresponding quantification data of P62, Beclin-1, Caspase-3, Bax and, LC3 in SH-SY5Y cells; GAPDH was used as an endogenous control. Continuous characteristics were compared using Student t-tests, and all the results are shown as the mean ± standard deviation (n = 3/group). Further, all experiments were repeated at least thrice. qRT-PCR, quantitative real-time polymerase chain reaction; NC, negative control. *p < 0.05. **p < 0.01, as compared with the NC inhibitor group. †p < 0.05. ††p < 0.01, as compared with the NC mimics group.

4. EA Attenuates Tissue Damage and Improves the Functional Status of Neuronal Cells and Motor Function in SCI Rats by Downregulating MiR-106b-5p

To explore further the function of miR-106b-5p in the neu-

roprotection of EA for SCIs, miR-106b-5p agomir or miR-106b-5p NC was administered immediately postsurgery. The expression level of miR-106b-5p in the injured spinal segment was significantly decreased after EA treatment in the SCI+EA group

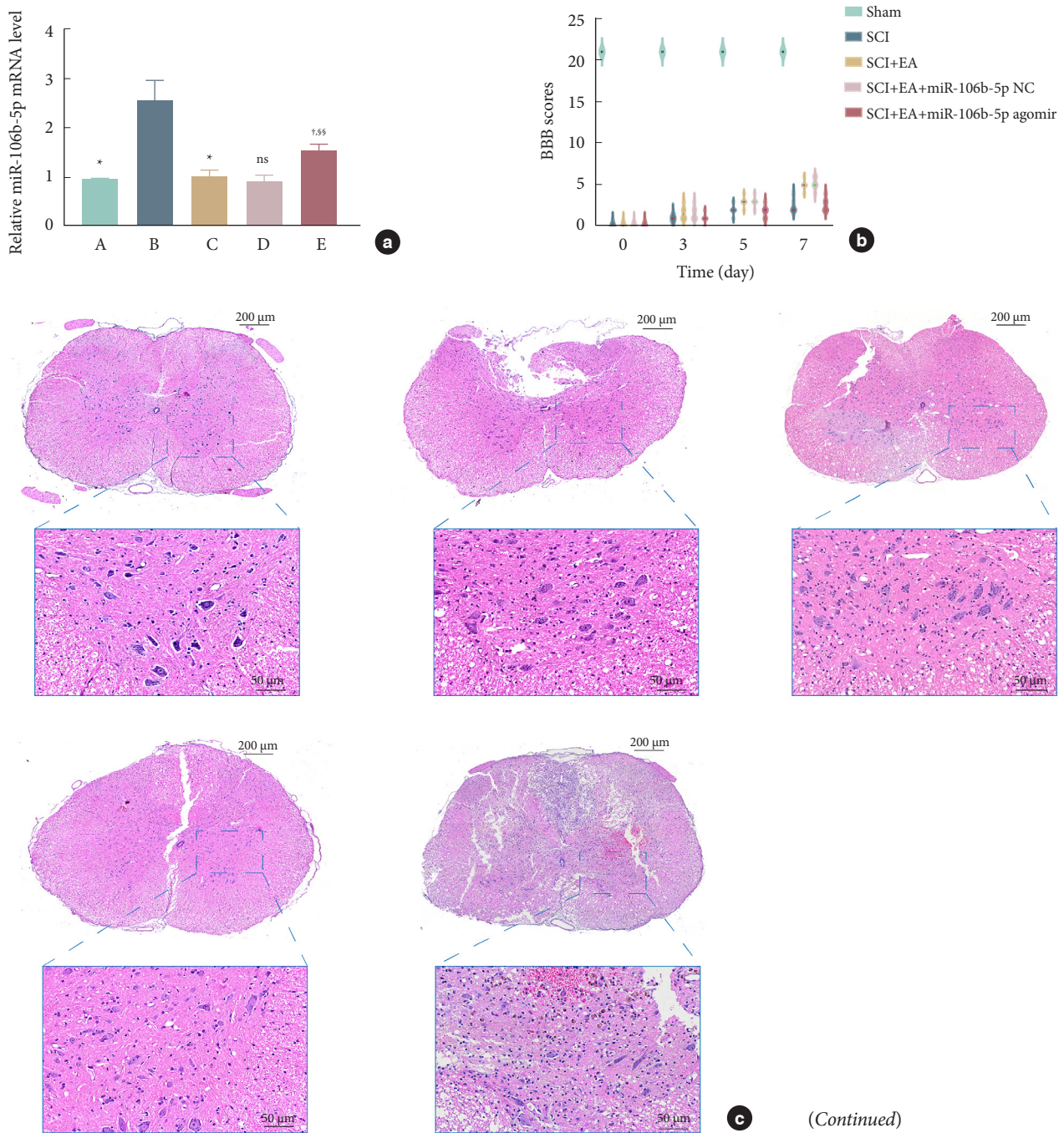


Fig. 5. Electroacupuncture (EA) alleviates spinal cord tissue damage and promotes motor function recovery after an spinal cord injury (SCI). (a) The expression of miR-106b-5p was confirmed by qRT-PCR in spinal tissue from different groups. (b) The BBB scores of rats in each group at various times, where a lower score indicates a more severe injury. (c) Representative HE-stained transverse sections (scale bars = 200 or 50 μm). (d) Observation of Nissl bodies in neurons of the spinal cord tissue of each group by Nissl staining (scale bars = 200 or 50 μm). Blue staining represents a Nissl body, where the darker the color of the Nissl bodies or the tabby shape, the better the neuronal state. qRT-PCR, quantitative real-time polymerase chain reaction; BBB, Basso-Beat-tie-Bresnahan locomotor scale; HE, hematoxylin and eosin. * $p < 0.05$, as compared with the SCI group. † $p < 0.05$. ^{ns} $p > 0.05$, as compared with the SCI+EA group. ^{§§} $p < 0.01$, as compared with the SCI+EA+miR-106b-5p NC group.

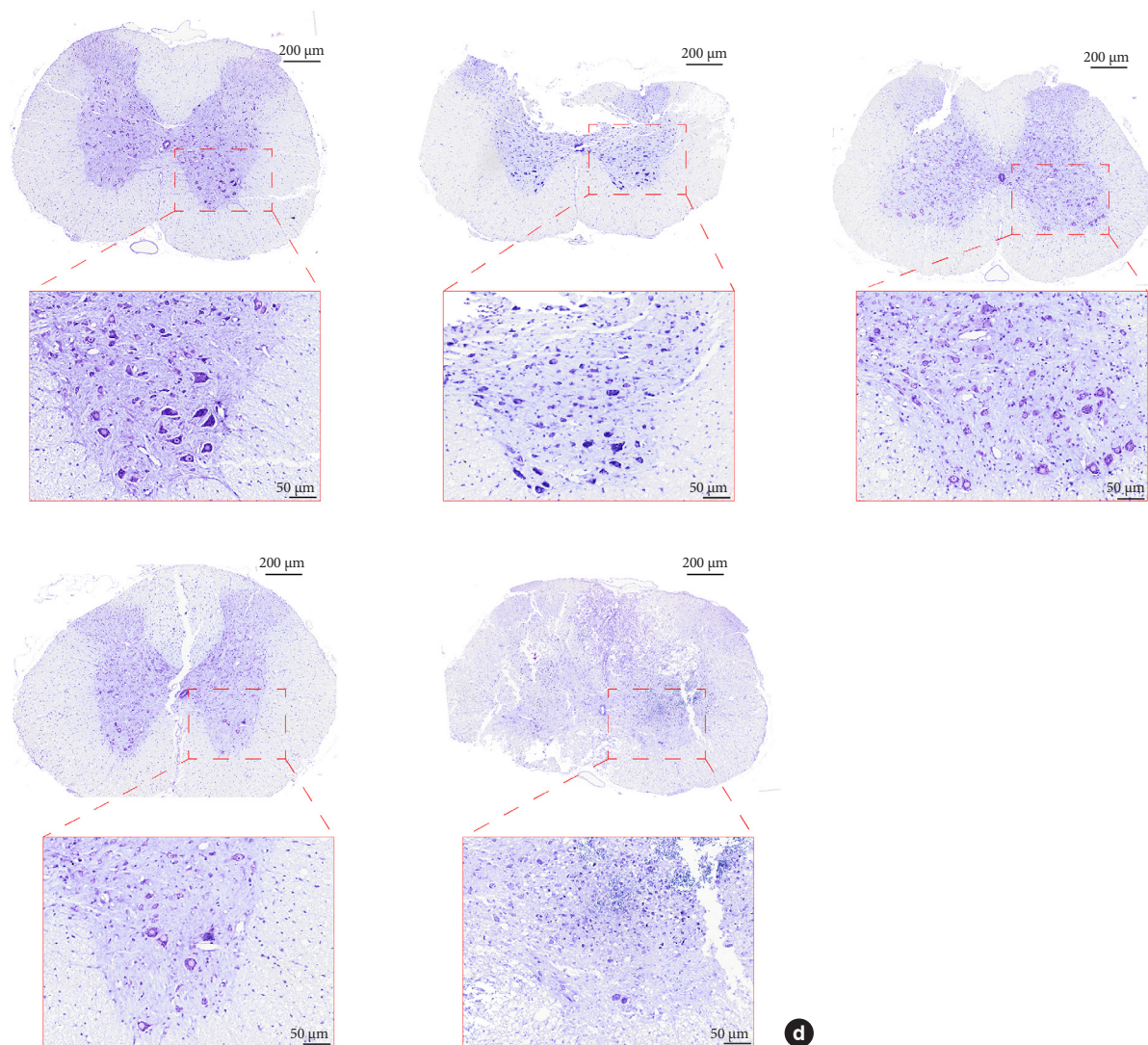


Fig. 5. Electroacupuncture (EA) alleviates spinal cord tissue damage and promotes motor function recovery after an spinal cord injury (SCI). (a) The expression of miR-106b-5p was confirmed by qRT-PCR in spinal tissue from different groups. (b) The BBB scores of rats in each group at various times, where a lower score indicates a more severe injury. (c) Representative HE-stained transverse sections (scale bars = 200 or 50 μm). (d) Observation of Nissl bodies in neurons of the spinal cord tissue of each group by Nissl staining (scale bars = 200 or 50 μm). Blue staining represents a Nissl body, where the darker the color of the Nissl bodies or the tabby shape, the better the neuronal state. qRT-PCR, quantitative real-time polymerase chain reaction; BBB, Basso-Beattie-Bresnahan locomotor scale; HE, hematoxylin and eosin. * $p < 0.05$, as compared with the SCI group. † $p < 0.05$. ^{ns} $p > 0.05$, as compared with the SCI+EA group. ^{ss} $p < 0.01$, as compared with the SCI+EA+miR-106b-5p NC group. (Continued)

compared to the SCI group ($p < 0.05$). However, miR-106b-5p agomir could significantly reverse the above-mentioned change in the SCI+EA+miR-106b-5p agomir group ($p < 0.05$) (Fig. 5a).

The BBB scale was utilized to investigate motor recovery, scores of which were similar among all groups before the SCI ($p > 0.05$), while scores in other groups were significantly lower than those in the sham group 1-day postsurgery (all $p < 0.01$). No significant differences were observed between the SCI and SCI+EA

groups on the third day postsurgery ($p > 0.05$), while the scores of the rats in the SCI+EA group were higher than those in the SCI group on the fifth ($p < 0.01$) and seventh ($p < 0.01$) days post-injury. However, the effect of EA treatment was reversed by the overexpression of miR-106b-5p, and the BBB score in the SCI+EA+miR-106b-5p agomir group was remarkably lower than those in the SCI+EA and SCI+EA+miR-106b-5p NC groups from 5 to 7 day postsurgery (all $p < 0.01$) (Fig. 5b, Table 2).

Table 2. BBB scores at various times pre- and postsurgery

Group (BBB score)	Before surgery	After surgery			
		0 Day	Third day	Fifth day	Seventh day
Sham	21.00 ± 0.00	21.00 ± 0.00	21.00 ± 0.00	21.00 ± 0.00	21.00 ± 0.00
SCI	21.00 ± 0.00	0.00 ± 0.00 ^{††}	1.00 ± 0.00	2.00 ± 0.58	2.50 ± 0.76
SCI+EA	21.00 ± 0.00	0.00 ± 0.00 ^{††}	1.67 ± 0.75	3.00 ± 0.58 ^{**§§}	5.00 ± 0.58 ^{**§§}
SCI+EA+miR-106b-5p NC	21.00 ± 0.00	0.00 ± 0.00 ^{††}	1.67 ± 0.75	3.00 ± 0.58 ^{§§}	5.17 ± 0.69 ^{§§}
SCI+EA+miR-106b-5p agomir	21.00 ± 0.00	0.00 ± 0.00 ^{††}	1.00 ± 0.58	1.83 ± 0.69	2.67 ± 0.75

Values are presented as mean ± standard deviation of 6 rats per group per time point, where lower BBB scores indicate poorer locomotor function. BBB, Basso-Beattie-Bresnahan locomotor scale; SCI, spinal cord injury; EA, electroacupuncture; NC, negative control.

One-way analysis of variance followed by least significant difference or Dunnett T3 *post hoc* test (where equal variances were not assumed) was applied for multiple comparisons.

^{††}*p* < 0.01, as compared with sham group. ^{**}*p* < 0.01, as compared with SCI group. ^{§§}*p* < 0.01, as compared with SCI+EA+miR-106b-5p agomir group.

H&E staining was used to identify changes in tissue structures, the results of which revealed that the spinal cord structure was intact, gray-white matter was clear, and cells were regular in the sham group. In contrast, the image of the SCI group showed a lesion cavity at the injury center and obvious signs of tissue swelling. After EA treatment, the spinal cord tissue loss and neuronal edema of the rats in the SCI+EA group were alleviated, and the gray-white matter structure and boundary became clearer. Collectively, these results demonstrated that EA played a role in SCI repair in rats. However, miR-106b-5p overexpression was able to reverse the effects of EA, such that the necrosis cavity and tissue edema were visible in the SCI+EA+miR-106b-5p agomir group and the number of neuronal cells significantly decreased when compared with the SCI+EA+miR-106b-5p NC group (Fig. 5c).

The Nissl staining results of the sham group indicate that neuronal structures were intact and clear, the nuclei were obvious and abundant, and Nissl bodies remained evenly distributed in the cytoplasm. In the SCI group, the neuronal cells appeared swollen with unclear structures, and the number of Nissl bodies decreased while the color became lighter. In the SCI+EA group, cell morphology improved and edema reduced in response to EA treatment, while the loss of Nissl bodies was significantly alleviated. However, neuronal cells showed morphological deterioration and significant swelling, and the number of Nissl bodies was decreased after the overexpression of miR-106b-5p in the SCI+EA+miR-106b-5p agomir group compared with the SCI+EA+miR-106b-5p NC group (Fig. 5d).

5. EA Facilitates Microstructure and Autophagosome Changes to Injured Spinal Cord Tissue

Ultrastructural changes to the spinal cord tissue were exam-

ined using TEM ($\times 3,000$ magnification). In the sham group, the structure of the nuclei and organelles was normal, and no autophagosomes and autolysosomes were observed (Fig. 6A). In the SCI group, the cells exhibited intracellular edema, and the number of lysosomes (yellow arrow) and autolysosome (green arrow) increased (Fig. 6B). Further, in the SCI+EA group, more autophagosomes (red arrow) and autolysosomes (green arrow) could be observed when compared with the SCI group (Fig. 6C), and in the SCI+EA+miR-106b-5p NC group, the number of autophagosomes (red arrow) was greater than that in the SCI group (Fig. 6D). Further, in the SCI+EA+miR-106b-5p agomir group, cells were swollen, and several lysosomes (yellow arrow) could be seen (Fig. 6E). These results illustrate how EA can enhance the autophagy flux, while the overexpression of miR-106b-5p can reverse the effects induced by EA.

6. EA Promotes Autophagy and Suppresses SCI-Induced Apoptosis by Downregulating MiR-106b-5p

The expressions of the autophagy-related proteins LC3, Beclin-1, and P62, as well as of the apoptotic-related proteins Bax and Caspase-3, in spinal cord tissues were detected by WB analysis. After normalization with the internal reference protein GAPDH or Tubulin, no significant difference was observed in the expression of Beclin-1 between the SCI and sham groups; meanwhile, the expressions of P62 (*p* < 0.01), Caspase-3 (*p* < 0.01), and Bax (*p* < 0.05) in the SCI group were significantly increased compared to those in the sham group. In addition, in comparison to the SCI group, EA decreased the expressions of P62 (*p* < 0.05), Caspase-3 (*p* < 0.01), and Bax (*p* < 0.05) and increased the ratio of LC3-II to LC3-I (*p* < 0.01) and the expression of Beclin-1 (*p* < 0.05). These results support the view that EA plays an important role in promoting autophagy and inhibiting apoptosis

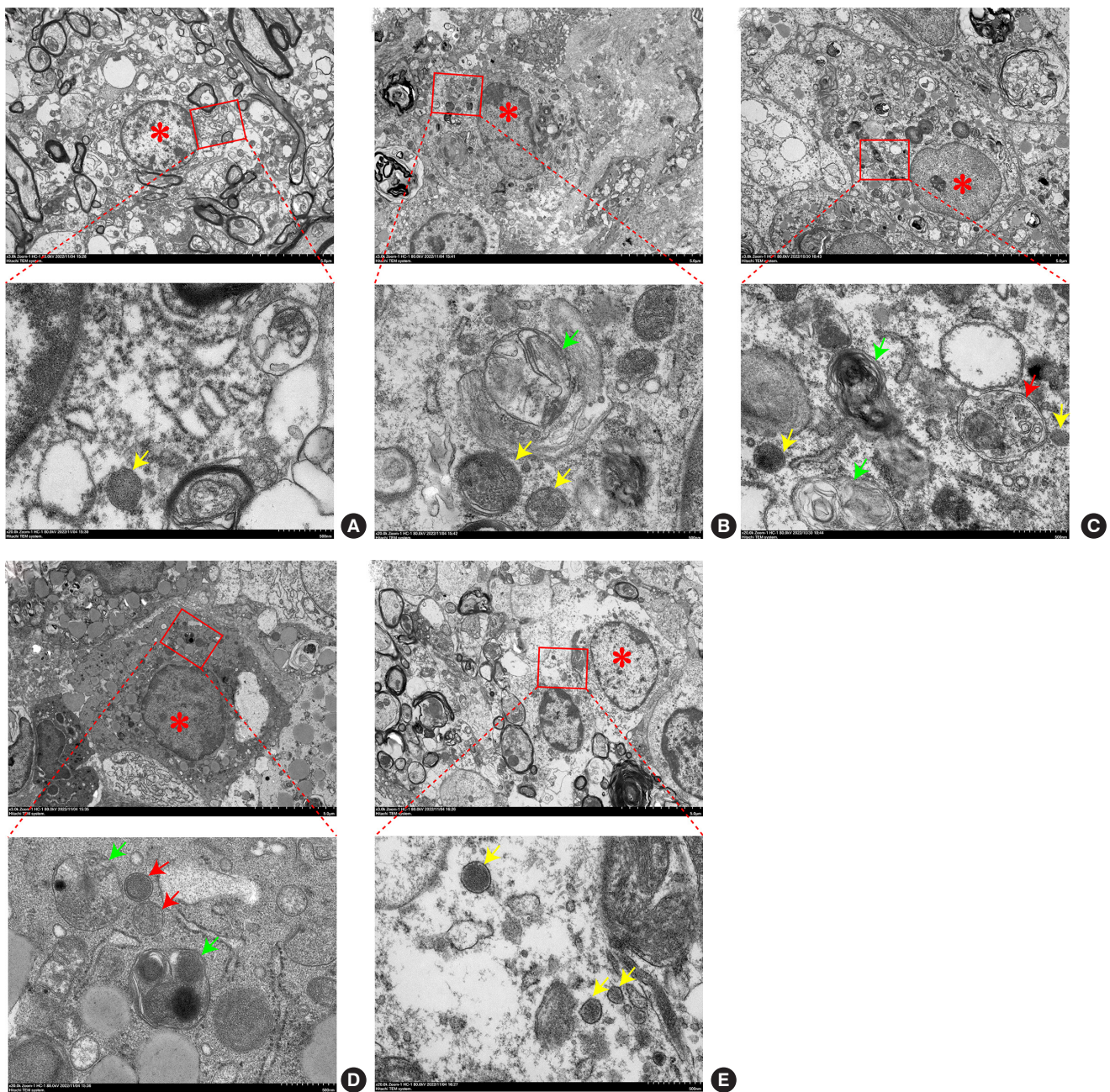


Fig. 6. Observation of microstructure and autophagosome changes in each group by transmission electron microscopy. (A) In the sham group, the nucleus was regular and intact, without autophagosomes and autolysosomes. (B) In the spinal cord injury (SCI) group, neurons showed swelling with vacuolization and karyopyknosis, and the number of lysosomes and autolysosomes increased. (C) In the SCI+EA group, the morphology of the nuclei was nearly normal; the mitochondria exhibited swelling to a lesser extent; and the number of the autophagosomes, and autolysosomes were increased. (D) In the SCI+EA+miR-106b-5p NC group, some autolysosomes, and autophagosomes can be found. (E) In the SCI+EA+miR-106b-5p agomir group, cell swelling, a pyknotic nucleus, and several lysosomes were observed. Scale bars = 5 μm and 500 nm. The red asterisk identifies the nucleus; the yellow arrow indicates lysosomes; the green arrow points to autolysosomes; the red arrow identifies autophagosomes. EA, electroacupuncture.

after an SCI. However, the overexpression of miR-106b-5p can reverse the changes induced by EA treatment ($p < 0.05$). No significant difference was found between the SCI+EA and the SCI+

EA+miR-106b-5p NC groups ($p > 0.05$) (Fig. 7), and the above expression patterns of Beclin-1, P62, Bax, and Caspase-3 were confirmed by qRT-PCR (Fig. 8) and immunohistochemical

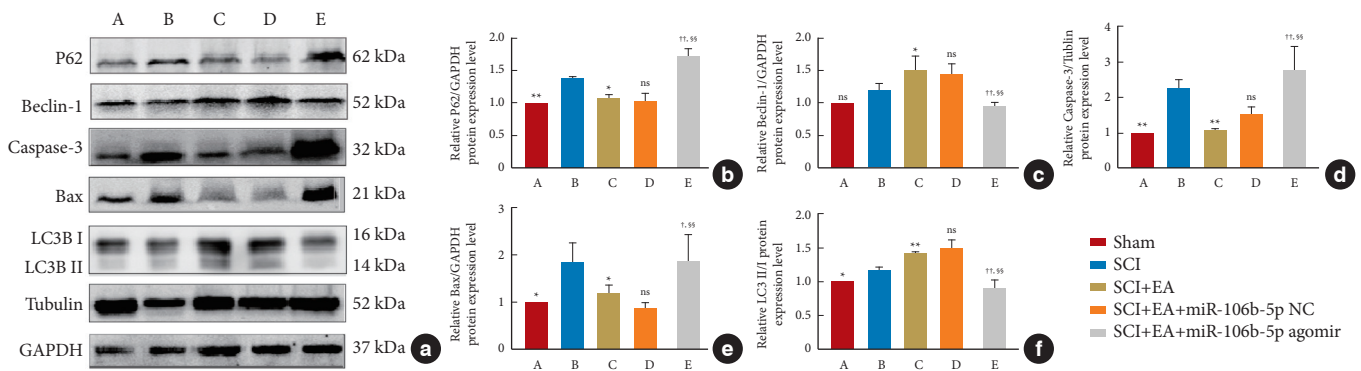


Fig. 7. Upregulating the miR-106b-5p expression reversed the effect of electroacupuncture (EA) in rats after a spinal cord injury (SCI) evaluated by Western blot assay. (a–f) Western blot assay and quantitative analysis of integrated optical densities for autophagy-related (P62 [b], Beclin-1 [c], LC3 [f]) and apoptosis-related (Bax [e] and Caspase-3 [d]) proteins; GAPDH or Tubulin was used as an endogenous control. One-way analysis of variance followed by least significant difference or Dunnett T3 *post hoc* test was used. All the results are shown as the mean ± standard deviation (n = 3/group). All experiments were repeated at least thrice. *p < 0.05. **p < 0.01. ^{ns}p > 0.05, as compared with the SCI group. †p < 0.05. ††p < 0.01. ^{ns}p > 0.05, as compared with the SCI+EA group. [§]p < 0.01, as compared with the SCI+EA+miR-106b-5p NC group.

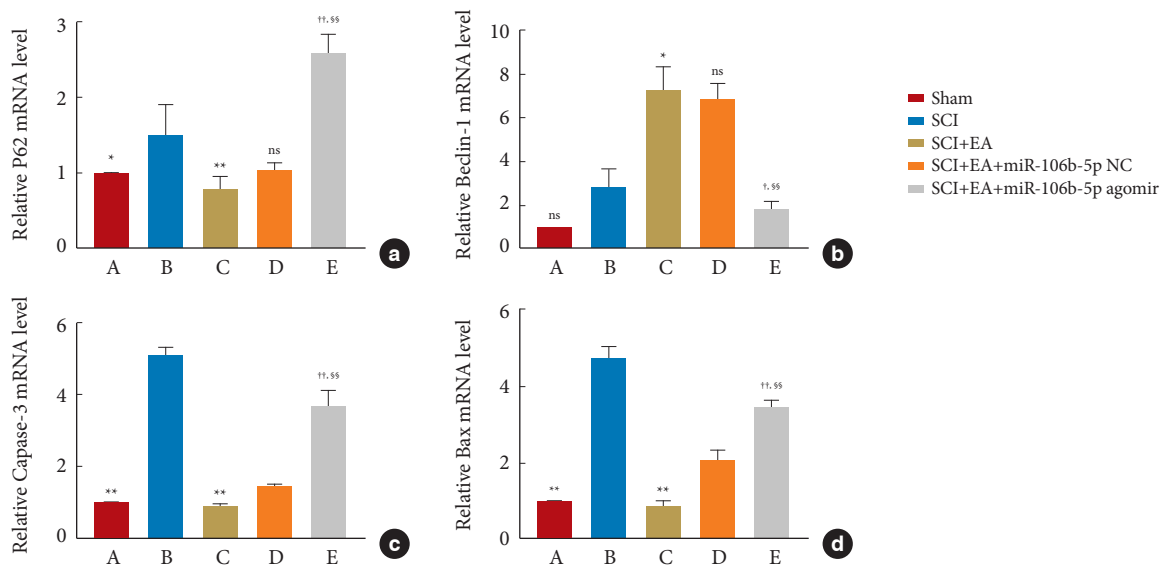


Fig. 8. Upregulating the miR-106b-5p expression reversed the effect of electroacupuncture (EA) in rats after the spinal cord injury (SCI) was evaluated by qRT-PCR. The mRNA levels of P62 (a), Beclin-1 (b), Caspase-3 (c), and Bax (d) were determined by qRT-PCR; GAPDH was selected as the internal reference. One-way analysis of variance followed by least significant difference or Dunnett T3 *post hoc* test was used. All the results are shown as the mean ± standard deviation (n = 3/group). All experiments were repeated at least thrice. qRT-PCR, quantitative real-time polymerase chain reaction. *p < 0.05. **p < 0.01, as compared with the SCI group. †p < 0.05. ††p < 0.01. ^{ns}p > 0.05, as compared with the SCI+EA group. [§]p < 0.05. ^{§§}p < 0.01, as compared with the SCI+EA+miR-106b-5p NC group.

staining (Fig. 9).

DISCUSSION

This is a novel study investigating the role of autophagy and apoptosis in the protection offered by EA treatment of SCIs. In

this experiment, we first found that the expression of miR-106b-5p was markedly increased after an SCI, and we subsequently determined that EA can regulate autophagy and apoptosis by suppressing the expression of miR-106b-5p. These data might contribute to a better understanding of the mechanism involved in EA treatment at the molecular level following an SCI and pro-

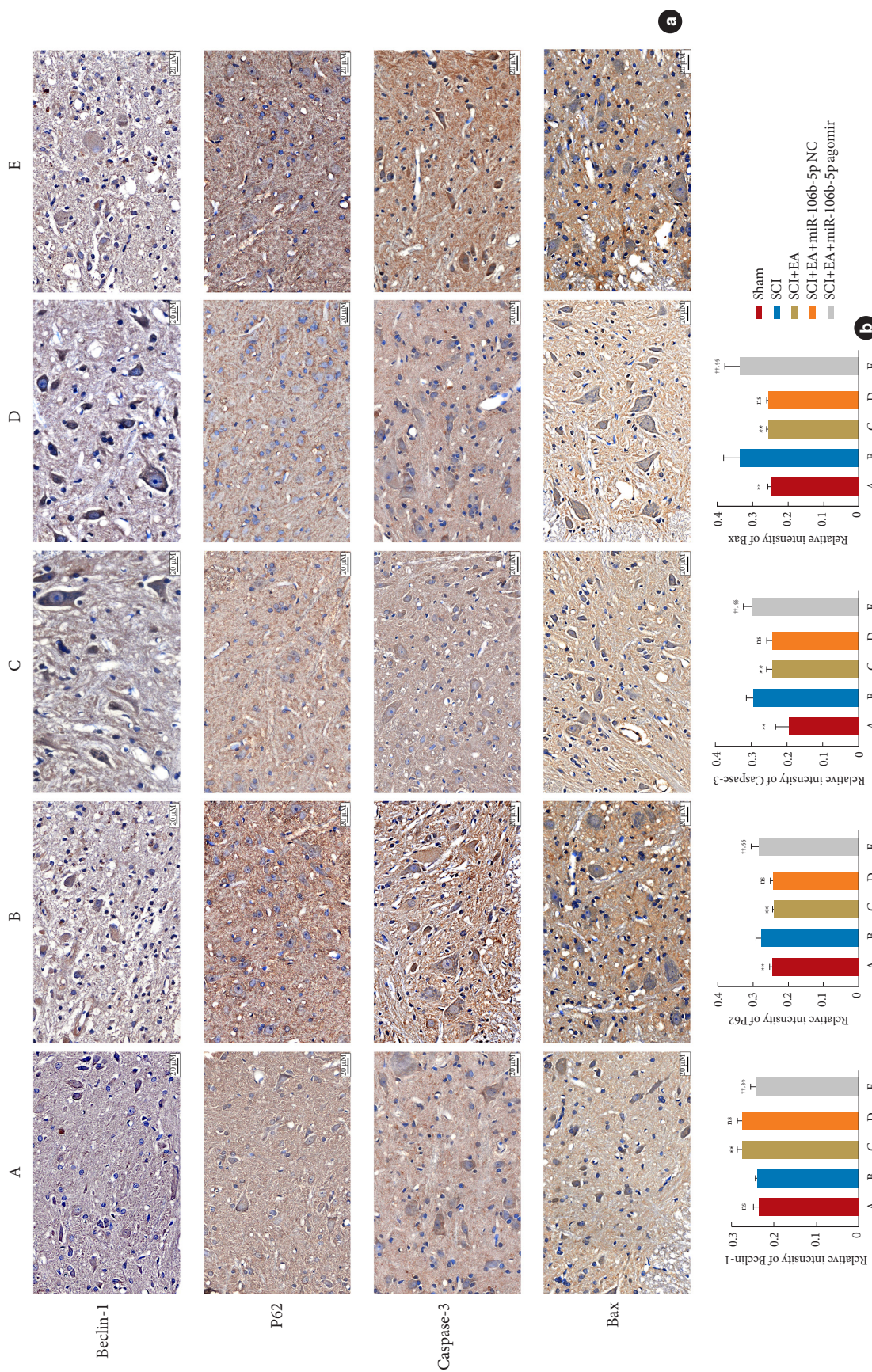


Fig. 9. Effects of EA in injured rat spinal cords evaluated by immunohistochemical staining for Beclin-1, P62, Caspase-3, and Bax proteins (scale bars = 20 μM). (b) Quantitative analysis of the mean optical density for these proteins. One-way analysis of variance followed by least significant difference or Dunnett T3 *post hoc* test was used. All the results are shown as the mean ± standard deviation (n = 3/group). All experiments were repeated at least 3 thrice. SCI, spinal cord injury; EA, electroacupuncture. **p < 0.01, as compared with the SCI group. ††p < 0.01, as compared with the SCI+EA group. †††p < 0.01, as compared with the SCI+EA+miR-106b-5p NC group.

vide a new therapeutic strategy for SCI treatment.

EA is a modified method based on traditional acupuncture combined with modern electrotherapy, and it has been examined as an important alternative and adjunctive treatment option for SCIs in recent years.²⁷ EA has been reported to have a variety of beneficial effects by stimulating special acupoints and conducting them from the meridians and channels to the target site.²⁸ The mechanisms of EA to create a better microenvironment for neuroprotection after an SCI may lead to reduced inflammatory responses and lipid peroxidation; apoptosis inhibition; regulated oxidative stress; enhanced autophagy; the promotion of neural stem cell proliferation, neuronal survival, and axonal regeneration; the activation of the propriospinal neuronal network; and more.²⁹ The selection of acupoints is a critical factor that can determine the efficacy of acupuncture.¹⁰ Previous studies have documented that the Jiaji (EX-B2) acupoint has a synergistic effect on reducing neuronal damage post-SCI by regulating autophagy and apoptosis.^{12,13} In addition, there is mounting evidence that EA at the Zusanli (ST36) acupoint promotes recovery from SCIs via the protection of nerve cells and the prevention of apoptosis in SCI rats.³⁰ Consistent with these results, our data also demonstrate that EA treatment at the Jiaji (EX-B2) and Zusanli (ST36) acupoints can increase BBB scores, improve the survival of motor neurons, and alleviate pathological tissue damage. Together, these results further verify that EA is an effective therapeutic means to restore motor function after an SCI.

As important regulators of normal nervous functions, miRNAs are closely related to morphological and functional changes in the nervous system.³¹ Following a SCI, the homeostasis of many miRNAs is disturbed, and the aberrantly dysregulated miRNAs can either alleviate or aggravate conditions after an SCI, as dictated by their downstream target genes.³² For example, miR-21 has been found to play an important role in limiting secondary neuronal apoptosis following an SCI,²⁴ while Zhou et al.³³ demonstrated that miR-27a can facilitate SCI recovery by regulating the autophagy flux for neuroprotection. Moreover, EA treatment of SCIs in rats induces changes to miRNA expression profiles, as also demonstrated in previous studies.³⁴ MiR-106b-5p, a member of the 106b-25 cluster and a paralogue of the 17-92 cluster,³⁵ has been well-studied in many diseases, including breast cancer,³⁵ and acute renal injury.³⁶ Recently, miR-106b-5p was found to be abnormally expressed in the spinal cords of mice models of neuropathic pain.⁴ The level of which in these diseases is markedly increased, while the knockdown miR-106b-5p expression can regulate apoptosis and autophagy,

as well as inhibit cell proliferation and induce cell cycle arrest.³⁵ However, relatively little is known regarding the regulatory role of miR-106b-5p in neurological functional recovery after SCI. In the current study, we validated a significantly increased miR-106b-5p expression in the blood of SCI patients and the spinal cord tissue of SCI rats, where apoptosis was inhibited, and autophagy was enhanced after downregulating miR-106b-5p through EA treatment, indicating that EA treatment has a regulative effect by inhibiting miR-106b-5p expression.

Appropriate autophagy activation has been proposed as an approach to nerve regeneration by reducing secondary injury.¹² Autophagy is a dynamic, multi-step process with several regulatory steps, including autophagy induction, vesicle nucleation, expansion, and autophagosome maturation and degradation. Beclin-1 is recognized as a regulator of autophagy and a key player in isolation membrane (also called a phagophore) formation, which signals the initiation of the autophagic process.³⁷ In this study, we demonstrated that miR-106b-5p can directly target the Beclin-1 gene using the dual-luciferase reporter assay. Further, LC3 plays a crucial role in promoting the expansion and maturation of autophagosomes,⁴ where, during autophagy activation, LC3-I in the cytoplasm is converted into LC3-II and recruited to the autophagosome membrane. Thus, a higher LC3-II to LC3-I ratio indicates an increased autophagy flow. Further, LC3-II can interact with P62, an autophagy cargo protein, the accumulation of which signals autophagy suppression.⁴ Previously, the inhibition of the autophagy flux was reported to contribute to neuronal cell damage in SCIs and to be associated with worse functional outcomes,³⁸ but in the present study, we found that EA treatment significantly increased the Beclin-1 expression and LC3-II to LC3-I ratio and decreased the P62 level in SCI rats, demonstrating increased functional autophagic flux under EA conditions. Moreover, autophagosome and autolysosome accumulation were observed by TEM following EA treatment, indicating that autophagic flux in the SCI+EA group was significantly enhanced.

Previous studies have found that the death of spinal cord neurons after an SCI occurs primarily via apoptosis, which is fundamental to the pathological mechanism of secondary injury, leading to permanent or long-term functional deficits following an SCI.¹² However, activating a suitable degree of autophagy to allow lysosomes to degrade damaged mitochondria can protect spinal cord neurons against SCI-induced apoptosis and can promote neuronal survival. Furthermore, autophagy can limit neuronal death by selectively reducing the abundance of proapoptotic proteins in the cytosol.⁴ Moreover, it has been revealed that

EA can contribute to functional recovery by attenuating SCI-induced Bax and Caspase-3 upregulation in injured spinal cords.^{13,31} In this study, our data show that an EA-enhanced autophagy flux was accompanied by inhibition in apoptosis, manifested as a gradual decrease in Bax and Caspase-3 levels. In addition, many studies have proven that EA can also create a better microenvironment to inhibit apoptosis by increasing microcirculation and blood flow, triggering the synthesis and secretion of neurotrophic factors, reducing the levels of pro-inflammatory cytokines, and so on.²⁹

To illustrate the underlying role of miR-106b-5p in EA treatment better, we next sought to treat rats using EA combined with injections of miR-106b-5p agomir. As expected, the overexpression of miR-106b-5p could reverse the effects of EA on autophagy and apoptosis. Thus, the regulation of autophagy and apoptosis induced by EA plays a vital role in promoting neuronal survival, accelerating nerve regeneration, and improving motor function after an SCI.^{12,29} Many studies have utilized cortical motor-evoked potentials, somatosensory evoked potentials, or neural tracing techniques to demonstrate EA's ability to promote neural circuitry reconstruction and functional recovery.^{39,40} In this study, we also observed via TEM and H&E staining that the inner environment in the injury segment and the ultrastructure of neurons were significantly improved after EA treatment. The results of Nissl staining further demonstrate that neuronal function and survival were significantly increased post-EA treatment. However, these protective effects of EA could be reversed by the overexpression of miR-106b-5p.

This study has some limitations. First, we did not perform a microarray analysis of spinal cord samples from SCI rats before and after EA treatment. Second, we did not use autophagy inhibitors to explore the effects of EA. Third, whether miR-106b-5p inhibitors affect motor function after an SCI remains unclear, and fourth, SH-SY5Y cells were chosen to mimic the SCI model *in vitro*, as they were identified as commonly used in human *in vitro* SCI research. Meanwhile, it is true that there exist differences between the SH-SY5Y cell line and the spinal cord, but it will be much more convincing if primary spinal cord neuronal cells or other neuronal cell lines were chosen to confirm our conclusion further. As such, future studies should identify the precise molecular and cellular mechanisms underlying the negative correlation between EA and motor dysfunction in SCIs.

CONCLUSION

In summary, EA can decrease the miR-106b-5p expression to

reverse remarkably the unfavorable microenvironment of the SCI segment by regulating autophagy and apoptosis, which is crucial for nerve regeneration and functional recovery. Thus, EA may have great potential applications in SCIs, and miR-106b-5p could be a potential therapeutic intervention following an SCI.

NOTES

Supplementary Materials: Supplementary Tables 1-2 can be found via <https://doi.org/10.14245/ns.2346446.223>.

Conflict of Interest: The authors have nothing to disclose.

Funding/Support: This study is supported by the National Natural Science Foundation of China (No. 81960417), Guangxi Key Research and Development Program (No. GuiKeAB20159027), Guangxi Natural Science Foundation (No. 2018GXNSFAA050033), and the Young Scientist Fund of the Natural Science Foundation of Guangxi (No. 2022GXNSFBA035545).

Acknowledgments: We would like to thank all the patients and control subjects who participated in the study for their consent and cooperation. We sincerely thank Professor Yiji Su and Ying Liu for their technical support.

Author Contribution: Conceptualization: SG, JC; Formal Analysis: SG; Investigation: YY; Methodology: XL, JC; Project Administration: YT, YG; Writing – Original Draft: JC; Writing – Review & Editing: JX.

ORCID

Shuhui Guo: 0000-0002-7643-437X

Jianmin Chen: 0000-0002-0528-5354

Ye Yang: 0000-0002-3831-2320

Xiaolu Li: 0009-0009-4673-2016

Yun Tang: 0000-0002-8217-5132

Yuchang Gui: 0000-0002-5966-2573

Jianquan Chen: 0009-0000-7581-5552

Jianwen Xu: 0000-0002-8095-591X

REFERENCES

1. Lee S, Nam H, Joo KM, et al. Advances in neural stem cell therapy for spinal cord injury: safety, efficacy, and future perspectives. *Neurospine* 2022;19:946-60.
2. Tabarestani TQ, Lewis NE, Kelly-Hedrick M, et al. Surgical considerations to improve recovery in acute spinal cord injury. *Neurospine* 2022;19:689-702.
3. Lai Z, Liu H, Liu G. Meta-analysis on the effects of electric acupuncture on neural functional recovery and related path-

- ways of rats after spinal cord injury. *Biomed Res Int* 2022;2022:8613384.
4. Gu Y, Chen D, Zhou L, et al. Lysine-specific demethylase 1 inhibition enhances autophagy and attenuates early-stage post-spinal cord injury apoptosis. *Cell Death Discov* 2021;7:69.
 5. Huang R, Wang S, Zhu R, et al. Identification of key eRNAs for spinal cord injury by integrated multinomial bioinformatics analysis. *Front Cell Dev Biol* 2021;9:728242.
 6. Wang SX, Lu YB, Wang XX, et al. Graphene and graphene-based materials in axonal repair of spinal cord injury. *Neural Regen Res* 2022;17:2117-25.
 7. Li Y, Lei Z, Ritzel RM, et al. Impairment of autophagy after spinal cord injury potentiates neuroinflammation and motor function deficit in mice. *Theranostics* 2022;12:5364-88.
 8. Shi Z, Yuan S, Shi L, et al. Programmed cell death in spinal cord injury pathogenesis and therapy. *Cell Prolif* 2021;54:e12992.
 9. Saraswat Ohri S, Bankston AN, Mullins SA, et al. Blocking autophagy in oligodendrocytes limits functional recovery after spinal cord injury. *J Neurosci* 2018;38:5900-12.
 10. Cao S, Yang Y, Yu Q, et al. Electroacupuncture alleviates ischaemic brain injury by regulating the miRNA-34/Wnt/autophagy axis. *Brain Res Bull* 2021;170:155-61.
 11. Zou J, Dong X, Wang K, et al. Electroacupuncture inhibits autophagy of neuron cells in postherpetic neuralgia by increasing the expression of miR-223-3p. *Biomed Res Int* 2021;2021:6637693.
 12. Hongna Y, Hongzhao T, Quan L, et al. Jia-Ji electro-acupuncture improves locomotor function with spinal cord injury by regulation of autophagy flux and inhibition of necroptosis. *Front Neurosci* 2020;14:616864.
 13. Liu J, Wu Y. Electro-acupuncture-modulated miR-214 prevents neuronal apoptosis by targeting Bax and inhibits sodium channel Nav1.3 expression in rats after spinal cord injury. *Biomed Pharmacother* 2017;89:1125-35.
 14. Tigchelaar S, He Z, Tharin S. Spinal cord injury: a study protocol for a systematic review and meta-analysis of microRNA alterations. *Syst Rev* 2022;11:61.
 15. He S, Wang Z, Li Y, et al. MicroRNA-92a-3p enhances functional recovery and suppresses apoptosis after spinal cord injury via targeting phosphatase and tensin homolog. *Biosci Rep* 2020;40:BSR20192743.
 16. Zhou J, Li Z, Zhao Q, et al. Knockdown of SNHG1 alleviates autophagy and apoptosis by regulating miR-362-3p/Jak2/stat3 pathway in LPS-injured PC12 cells. *Neurochem Res* 2021;46:945-56.
 17. Zhou Z, Hu B, Lyu Q, et al. miR-384-5p promotes spinal cord injury recovery in rats through suppressing of autophagy and endoplasmic reticulum stress. *Neurosci Lett* 2020;727:134937.
 18. Segaran RC, Chan LY, Wang H, et al. Neuronal development-related miRNAs as biomarkers for Alzheimer's disease, depression, schizophrenia and ionizing radiation exposure. *Curr Med Chem* 2021;28:19-52.
 19. Camkurt MA, Karababa F, Erdal ME, et al. Investigation of dysregulation of several microRNAs in peripheral blood of schizophrenia patients. *Clin Psychopharmacol Neurosci* 2016;14:256-60.
 20. Li H, Quan F, Zhang P, et al. Long non-coding RNA SNHG16, binding with miR-106b-5p, promoted cell apoptosis and inflammation in allergic rhinitis by up-regulating leukemia inhibitory factor to activate the JAK1/STAT3 signaling pathway. *Hum Exp Toxicol* 2021;40(12_suppl):S233-45.
 21. Xiong Y, Xia Y, Deng J, et al. Direct peritoneal resuscitation with pyruvate protects the spinal cord and induces autophagy via regulating PHD2 in a rat model of spinal cord ischemia-reperfusion injury. *Oxid Med Cell Longev* 2020;2020:4909103.
 22. Zhou Y, Su P, Pan Z, et al. Combination therapy with hyperbaric oxygen and erythropoietin inhibits neuronal apoptosis and improves recovery in rats with spinal cord injury. *Phys Ther* 2019;99:1679-89.
 23. Hu R, Xu H, Jiang Y, et al. EA Improves the motor function in rats with spinal cord injury by inhibiting signal transduction of semaphorin3A and upregulating of the peripheral nerve networks. *Neural Plast* 2020;2020:8859672.
 24. Zhang T, Ni S, Luo Z, et al. The protective effect of microRNA-21 in neurons after spinal cord injury. *Spinal Cord* 2019;57:141-9.
 25. Fan Y, Wu Y. Tetramethylpyrazine alleviates neural apoptosis in injured spinal cord via the downregulation of miR-214-3p. *Biomed Pharmacother* 2017;94:827-33.
 26. Basso DM, Beattie MS, Bresnahan JC. A sensitive and reliable locomotor rating scale for open field testing in rats. *J Neurotrauma* 1995;12:1-21.
 27. Li K, Liu J, Song L, et al. Effect of electroacupuncture treatment at dazhui (GV14) and mingmen (GV4) modulates the PI3K/AKT/mTOR signaling pathway in rats after spinal cord injury. *Neural Plast* 2020;2020:5474608.
 28. Xiao X, Deng Q, Zeng X, et al. Transcription profiling of a revealed the potential molecular mechanism of governor vessel electroacupuncture for spinal cord injury in rats. *Neurospine* 2022;19:757-69.

29. Wu MF, Zhang SQ, Liu JB, et al. Neuroprotective effects of electroacupuncture on early- and late-stage spinal cord injury. *Neural Regen Res* 2015;10:1628-34.
30. Ding LL, Hu SF, He XW, et al. Warm acupuncture therapy alleviates neuronal apoptosis after spinal cord injury via inhibition of the ERK signaling pathway. *J Spinal Cord Med* 2023;46:798-806.
31. Zhu Y, Wu Y, Zhang R. Electro-acupuncture promotes the proliferation of neural stem cells and the survival of neurons by downregulating miR-449a in rat with spinal cord injury. *EXCLI J* 2017;16:363-74.
32. Ma L, Ma L, Yang Y, et al. Electroacupuncture-regulated miR-34a-3p/PDCD6 axis promotes post-spinal cord injury recovery in both in vitro and in vivo settings. *J Immunol Res* 2022;2022:9329494.
33. Zhou Q, Feng X, Ye F, et al. miR-27a promotion resulting from silencing of HDAC3 facilitates the recovery of spinal cord injury by inhibiting PAK6 expression in rats. *Life Sci* 2020;260:118098.
34. Zhou Z, Li H, Li H, et al. Comprehensive analysis of the differential expression profile of microRNAs in rats with spinal cord injury treated by electroacupuncture. *Mol Med Rep* 2020;22:751-62.
35. Farré PL, Duca RB, Massillo C, et al. MiR-106b-5p: a master regulator of potential biomarkers for breast cancer aggressiveness and prognosis. *Int J Mol Sci* 2021;22:11135.
36. Hu JM, He LJ, Wang PB, et al. Antagonist targeting miR-106b-5p attenuates acute renal injury by regulating renal function, apoptosis and autophagy via the upregulation of TCF4. *Int J Mol Med* 2021;48:169.
37. Hsu WT, Chen YH, Yang HB, et al. Electroacupuncture improves motor symptoms of Parkinson's disease and promotes neuronal autophagy activity in mouse brain. *Am J Chin Med* 2020;48:1651-69.
38. Li X, Zhan J, Hou Y, et al. Coenzyme Q10 regulation of apoptosis and oxidative stress in H₂O₂ induced BMSC death by modulating the Nrf-2/NQO-1 signaling pathway and its application in a model of spinal cord injury. *Oxid Med Cell Longev* 2019;2019:6493081.
39. Ding Y, Yan Q, Ruan JW, et al. Bone marrow mesenchymal stem cells and electroacupuncture downregulate the inhibitor molecules and promote the axonal regeneration in the transected spinal cord of rats. *Cell Transplant* 2011;20:475-91.
40. Yang Y, Xu HY, Deng QW, et al. Electroacupuncture facilitates the integration of a grafted TrkC-modified mesenchymal stem cell-derived neural network into transected spinal cord in rats via increasing neurotrophin-3. *CNS Neurosci Ther* 2021;27:776-91.

Supplementary Table 1. Primer sequence for quantitative real-time polymerase chain reaction

Primer	Forward (5'-3')	Reverse (3'-5')
rno-miR-106b-5p	CCAAGTGCTGACAGTGCAGATAA	mRQ 3' primer (Takara, Japan)
rno-Bax	TGGCGATGAACTGGACAACAA	GGGAGTCTGTATCCACATCAGCA
rno-Caspase-3	GAGACAGACAGTGGAACTGACGATG	GGCGCAAAGTGAAGTGGATGA
rno-Bcl-2	GCTCCTATTCCATCAAAACCCA	GTGAGGACACCCAAGCAAGAC
rno-P62	TGAAGGCTATTACAGCCAGAGTCAA	CCTTCAGTGATGGCCTGGTC
rno-U6	GGAACGATACAGAGAAGATTAGC	TGGAACGCTTCACGAATTTGCG
rno-GAPDH	GGCACAGTCAAGGCTGAGAATG	ATGGTGGTGAAGACGCCAGTA
hsa-miR-106b-5p	TGCGGCAACACCAGTTCGATGG	mRQ 3' primer (Takara, Japan)
hsa-Bcl-2	CCAGATGCGTTATGCCAGAC	CATTCATTCACGGGAACAC

Supplementary Table 2. Demographic details of the participants

No.	SCI patient						Healthy control	
	Age (yr)	Sex	ASIA	Etiology	Injury level	Duration (mo)	Age (yr)	Sex
1	33	M	B	Traumatic	L	1	32	M
2	44	M	D	Traumatic	L	1	40	M
3	34	M	D	Traumatic	L	5	28	M
4	38	M	C	Traumatic	C	4	36	M
5	25	F	D	Traumatic	L	3	24	F
6	34	M	D	Traumatic	C	6	26	M
7	67	F	B	Traumatic	T	1	60	F
8	57	F	C	Traumatic	C	3	54	F
9	25	M	C	Traumatic	C	4	26	M
10	27	M	D	Traumatic	L	4	28	M

SCI, spinal cord injury; ASIA, American Spinal Injury Association; Injury level: C, cervical; T, thoracic; L, lumbar.